Mitigation of Instabilities in a Z-Pinch Plasma by a Preembedded Axial Magnetic Field

Dimitry Mikitchuk, Christine Stollberg, Ramy Doron, Eyal Kroupp, Yitzhak Maron, Henry R. Strauss, Alexander L. Velikovich, and John L. Giuliani

***Abstract*— The effects of an axial magnetic field on the development of instabilities during a z-pinch implosion are studied using 2-D images and interferometry. The measurements clearly show mitigation of magneto Rayleigh–Taylor instabilities with increased magnitude of the preembedded axial magnetic field. Introducing the axial magnetic field also gives rise to new structures, indicating an interaction between the azimuthal and axial fields.**

***Index Terms*— Magnetic field effects, optical imaging, plasma pinch, plasma stability.**

THE z-pinch implosion is characterized by the development of magneto Rayleigh–Taylor (MRT) instabilities that perturb the plasma symmetry and subsequently disrupt the current flowing in the plasma, leading to reduced density and temperature at stagnation [1]. Therefore, the mitigation of such instabilities is essential for achieving optimized implosions for z-pinch applications such as inertial confinement fusion [2] and X-ray source development [3]. Recently, experiments on the stabilizing effect of an axial magnetic field on magnetically driven liner implosions have been done on Z facility at Sandia National Laboratories. Their results, undoubtedly encouraging, are far from being fully understood [4], which underscores the need for more research.

The present research focuses on a systematic study of the effects of an axial magnetic field on the evolution of instabilities during the implosion of a gas-puff z-pinch.

The experimental setup employs a z-pinch configuration with a preembedded, nearly uniform axial magnetic field of up to 0.5 T. The axial magnetic field is generated by a pair of Helmholtz coils, each of a radius of 50 mm, driven by a slow (rise time $\approx$5 ms) capacitor. A hollow, cylindrical Ar-gas load is injected into a 10-mm anode–cathode gap. The gas has an outer diameter of 38 mm and mass per length of 30 μg/cm. The implosion is driven by a 1.6-μs rise time, 300-kA discharge current pulse.

Manuscript received November 11, 2013; revised March 14, 2014; accepted May 24, 2014. Date of publication June 16, 2014; date of current version October 21, 2014. This work was supported by the U.S.-Israel Binational Science Foundation under Grant 2012096 and by the DOE-Cornell University Excellence Center (U.S.).

D. Mikitchuk, C. Stollberg, R. Doron, E. Kroupp, and Y. Maron are with the Weizmann Institute of Science, Rehovot 76100, Israel (e-mail: dimitry.mikitchuk@weizmann.ac.il; christine.stollberg@weizmann.ac.il; ramy.doron@weizmann.ac.il; eyal.kroupp@weizmann.ac.il; yitzhak.maron@weizmann.ac.il).

H. R. Strauss is with HRS Fusion, West Orange, NJ 07052 USA (e-mail: hank@hrsfusion.com).

A. L. Velikovich and J. L. Giuliani are with the Plasma Physics Division, Naval Research Laboratory, Washington, DC 20375 USA (e-mail: sasha.velikovich@nrl.navy.mil; john.giuliani@nrl.navy.mil).

Digital Object Identifier 10.1109/TPS.2014.2327094

The effect of the axial magnetic field on the plasma implosion is studied systematically for various initial field magnitudes. The 2-D imaging and interferometry are used for the plasma diagnostics. Filtered 2-D images of the visible plasma self-emission (bandpass 4000–6000 Å) are obtained from the radial direction by an intensified charged coupled device camera with a gate time of 3 ns. Interferometric measurements are performed with a Michelson-type interferometer, utilizing the second harmonic (532 nm) of a Q-switched Nd:YAG laser with a pulse duration of 7 ns.

Fig. 1 presents the 2-D and interferometric images of the plasma with different initial axial magnetic field strengths at the same stage of compression, i.e., when the plasma column is imploded to a radius of $\approx$8 mm. In the left column, Fig. 1(a), (c), and (e) show 2-D images for initial axial magnetic field strengths of $B_{z,0} = 0$, 0.2, and 0.4 T, respectively. From spectroscopic measurements (not presented here), we know that at the stage of the implosion presented in Fig. 1 the plasma consists mainly of Ar III and Ar IV ions, which do not have significant line emission in the spectral range recorded in the 2-D images. Therefore, the light intensity is mainly due to the continuum radiation that is proportional to the electron density squared and depends weakly on the temperature. The right column [Fig. 1(b), (d), and (f)] gives the corresponding interferograms. The displacement of the fringe positions is proportional to the line integral of the electron density along the laser beam path.

The introduction of an axial magnetic field has various effects on the plasma dynamics. The implosion is slowed down significantly by the magnetic pressure that builds up due to the compression of the preembedded axial magnetic field by the imploding plasma. In addition, the radius of the stagnating plasma (not shown here) increases with increasing initial axial magnetic field. Fig. 1 demonstrates the mitigation of the MRT instabilities with increasing initial axial magnetic field magnitude. Without the axial magnetic field, the 2-D measurement [Fig. 1(a)] shows clear instabilities on the edge of the plasma image [5], whereas the interferogram [Fig. 1(b)] proves that they are not limited to the observed edge of the 2-D image. This type of instability is mitigated by the introduction of the axial magnetic field of initial $B_{z,0} = 0.2$ T [Fig. 1(c) and (d)]. An increase of the axial magnetic field further reduces this type of asymmetries [Fig. 1(e) and (f)].

While the axial magnetic field mitigates, the MRT instabilities during the implosion, other phenomena appear only in its presence. The shape of the implosion is changed in Fig. 1(c)–(f), and there is nonaxisymmetric filamentation. The latter is especially strong near stagnation as seen in

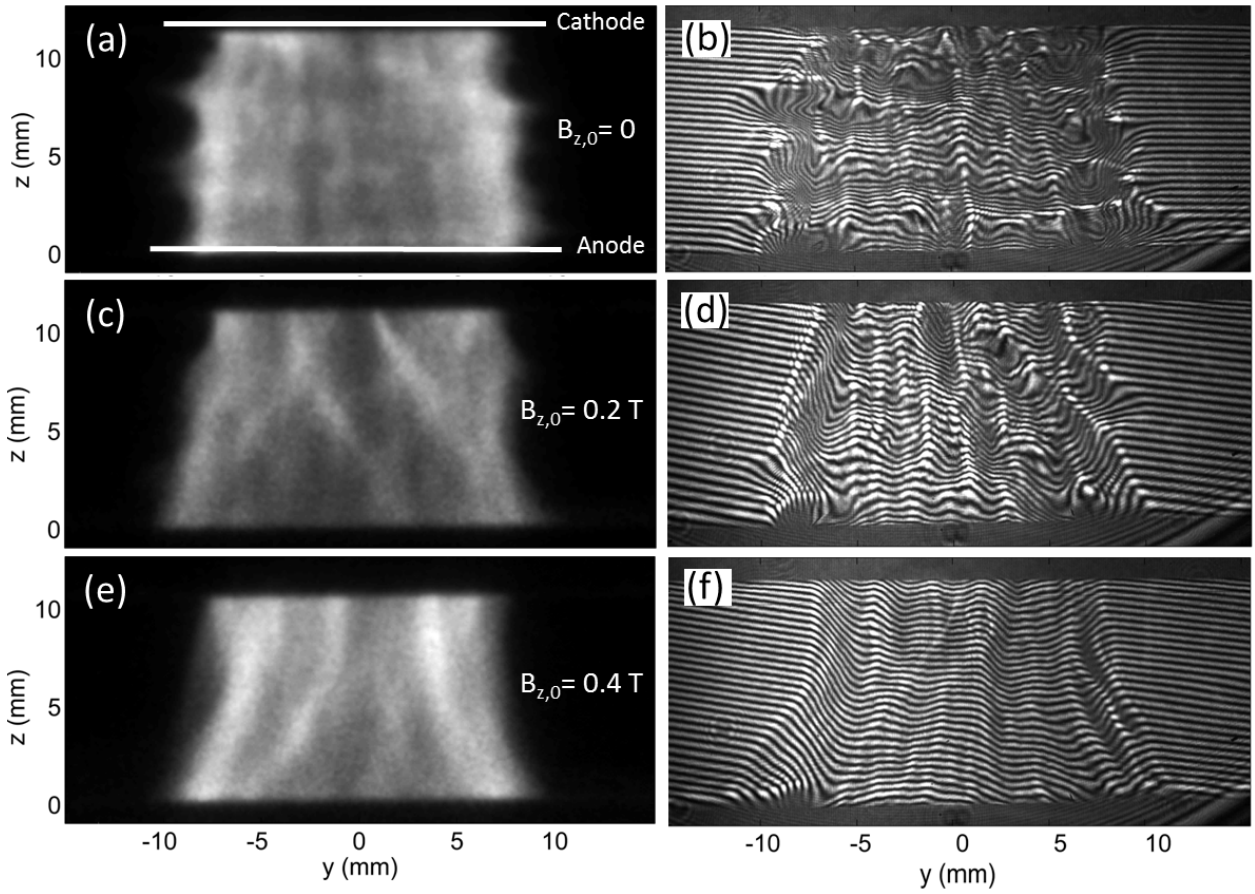

Fig. 1. 2-D images (left) and interferograms (right) of a self imploding plasma column with different preembedded axial magnetic fields. (a) and (b) $B_{z,0} = 0$, $t \approx 830$ ns. (c) and (d) $B_{z,0} = 0.2$ T, $t \approx 900$ ns. (e) and (f) $B_{z,0} = 0.4$ T, $t \approx 1030$ ns. The time $t = 0$ corresponds to the beginning of the pinch current (when the radius is 19 mm). All the data are recorded during inward acceleration, when the plasma column has imploded to $r \approx 8$ mm.

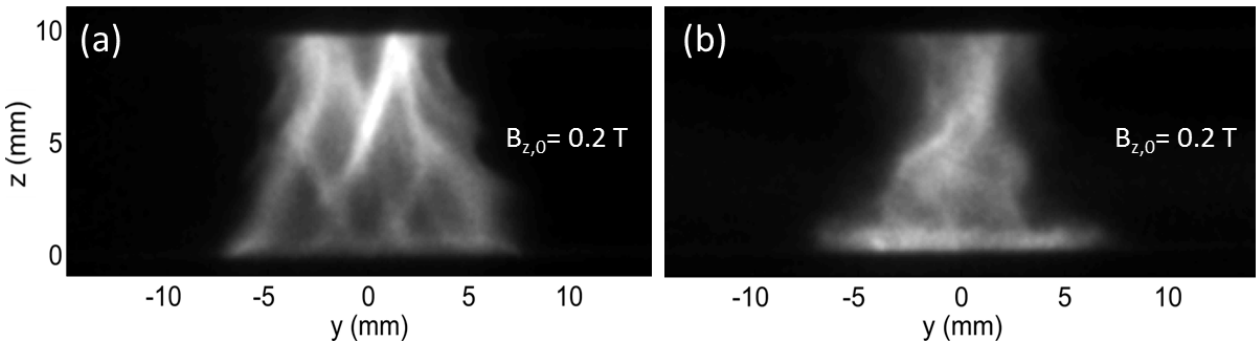

Fig. 2. Phenomena observed when an axial magnetic field is applied. (a) Non-axisymmetric filamentation at $t = 850$ ns (≈80 ns before stagnation). (b) Twisted plasma column at $t = 1260$ ns (≈200 ns after stagnation). We note that the image in (a) is recorded for a discharge current that is ≈20% higher than the currents in Fig. 1 and (b), leading to an earlier stagnation time. Although less prominent, the formation of filamentation is also observed at the lower current experiments.

Fig. 2(a). Long after stagnation [Fig. 2(b)], the plasma appears to be twisted, apparently following the geometry of the magnetic field.

REFERENCES

[1] D. D. Ryutov, M. S. Derzon, and M. K. Matzen, "The physics of fast Z pinches," *Rev. Modern Phys.*, vol. 72, no. 1, p. 167, 2000.

[2] S. A. Slutz *et al.*, "Pulsed-power-driven cylindrical liner implosions of laser preheated fuel magnetized with an axial fields," *Phys. Plasmas*, vol. 17, no. 5, p. 056303, 2010.

[3] S. A. Chaikovsky *et al.*, "The K-shell radiation of a double gas puff z-pinch with an axial magnetic field," *Laser Particle Beams*, vol. 21, no. 2, pp. 255–264, 2003.

[4] T. J. Awe *et al.*, "Observations of modified three-dimensional instability structure for imploding z-pinch liners that are premagnetized with an axial field," *Phys. Rev. Lett.*, vol. 111, no. 23, p. 235005, 2013.

[5] D. B. Sinars *et al.*, "Measurements of magneto-Rayleigh–Taylor instability growth during the implosion of initially solid metal liners," *Phys. Plasmas*, vol. 18, no. 5, p. 056301, 2011.